

8004

**The effect of flow
characteristics on sweet
corrosion in high-pressure,
three-phase, oil/water/gas
horizontal pipelines**

by Professor W Paul Jepson

Corrosion in Multiphase Systems Center, Ohio University, Athens, OH, USA

Prevention of Pipeline Corrosion Conference

Marriott Houston Westside Hotel
Houston, Texas

October 17-20, 1994

Organized by
Pipe Line Industry
and
Pipes & Pipelines International

4008

THE EFFECT OF FLOW CHARACTERISTICS ON SWEET CORROSION IN HIGH-PRESSURE, THREE-PHASE, OIL/WATER/GAS HORIZONTAL PIPELINES

EXPERIMENTShave been performed in large-diameter horizontal flow systems, and the effects of flow regime, oil/water composition, flow velocity, carbon dioxide partial pressure, and temperature on corrosion have been observed. The flow patterns in horizontal flow are different from vertical flow, and produce stratification of the liquid phases. The distribution of the phases is very important in horizontal multi-phase flows. Water layers at the bottom of the pipe were found even in slug flow.

The corrosion rates have been found to increase with an increase in the carbon dioxide partial pressure and flow velocity. For the oils considered, at oil compositions up to 60%, the oil/water mixture separated and a water layer flowed along the bottom of the pipe with the oil flowing above it. The corrosion rate did not change much for oil concentrations up to 60%. Above this value, the phases became well mixed, with oil being the continuous phase and the corrosion rates rapidly decrease to negligible amounts.

As the temperature was increased, the corrosion rate increased. A maximum in corrosion rate between 60 and 80°C was only noticed for the flow of saltwater alone. When oil was present or for slug flow conditions, no maximum in corrosion rate was observed for temperatures up to 90°C.

In slug flow, pulses of bubbles impact on the bottom of the pipe and evidence of bubble collapse has been found. This leads to high levels of corrosion and can produce holes in existing inhibitor films.

INTRODUCTION

Oil and gas wells are more frequently being located at remote places, e.g. subsea. Here, it is usually impractical to separate the oil, water, and gas at each well site. The products from several wells are usually combined and passed into a single, large-diameter, multi-phase pipeline and transported to platforms or gathering stations where the phases are separated. As the well depletes, enhanced-oil-recovery methods are employed. These often lead to substantial increases in the water cut and carbon dioxide levels in produced fluids. This multi-phase flow can cause

severe corrosion problems in these flowlines. Repair and maintenance work on these pipelines can be difficult and extremely expensive.

In an attempt to reduce the levels of corrosion, the injection of corrosion inhibitors, surfactants, and drag-reducing agents is commonly used. This has met with some success, but in many instances the corrosion rate is not diminished. This may be attributed to the effectiveness of these chemicals being dependent on the particular flow environment and conditions.

Corrosion and the effectiveness of inhibitors have been studied extensively using stirred beakers, rotating-cylinder electrodes, autoclaves, and small-diameter, single-phase flow facilities. Few of these methods take into account the effect of the hydrocarbon in the multi-phase mixture, and even less account of the effect of flow regime and velocity.

When a vertical flow system is utilized, the individual phases are thoroughly mixed and this often results in a homogeneous type of flow. This is not the case in horizontal flow, where the effect of gravity tends to lead to stratification of the phases. At the bottom of the pipe, a water layer is often present, with oil flowing above it. Further, very different flow regimes exist in horizontal pipelines. Lee, Sun, and Jepson (1993) identified the regimes occurring in three-phase horizontal flows. They also showed that the extra liquid phase has a great effect on the flow regime transitions. At low liquid and gas velocities, smooth and wavy stratified flows occur.

Slug flow, which is an intermittent flow regime, is observed at higher gas velocities. Here, fast-moving, aerated, slugs of liquid move down the pipe with pockets of gas between them. The front of the slug is a highly turbulent, mixing zone where gas is entrained. Sun and Jepson (1992), and Zhou and Jepson (1994), indicate the presence of regions of high wall-shear stress at the bottom of the pipe. This leads to high levels of corrosion there.

These flow effects are not accounted for in the methods mentioned above. It is, therefore, unwise to apply results generated from vertical flows or stirred beakers, etc., to horizontal multi-phase flows. Annular flows are observed for high gas and liquid velocities.

Green, Johnson and Choi (1989) have shown that flow regimes have a significant effect on corrosion rates. Stratified flow showed lower corrosion rates than slug flow. In slug flow, instantaneous values were several orders of magnitude higher when the slug passed by. They point out that it is essential to understand the flow in each regime and relate it to any corrosion studies.

Videm and Dugstad (1989) showed that iron concentration in the solution played an important role in the reaction chemistry. They observed that corrosion took place when FeCO_3 is soluble in solution and no protective carbonate film is formed. The corrosivity of the solution increased when the iron concentration was low. The protection that an Fe^{2+} film offered depended on the temperature of the solution, and a stable film formed only at temperatures exceeding 50°C . This protection was found to increase if the pH was low and no alkaline substances were present in the solution. In later work (1994), they showed that corrosion product layers are removed by the stresses caused by the flow.

Mishra, Olson, Al-Hassan and Salama (1992), and Dugstad (1992), also found that iron carbonate film formation has an effect on corrosion. The former showed that temperature, pH, carbon dioxide partial pressure, brine content, material composition, and flow velocity affected corrosion and protective carbonate film formation. The latter focussed on the influence of temperature and steel to water ratio on the precipitation kinetics and the saturation and supersaturation of iron carbonate.

Several models for predicting corrosion rates have been developed. De Waard and Milliams (1975) performed tests in a stirred beaker to determine the effect of carbon dioxide partial pressure and temperature on corrosion. Their results indicated that the corrosion rate increased with an increase of both partial pressure and temperature. Later, De Waard, Lotz, and Milliams (1991) created a model to predict a 'worst case' corrosion rate. The effect of liquid velocity on corrosion rate was appended by De Waard and Lotz (1993).

Efird, Wright, Boros and Hailey (1993) related laboratory corrosion data to the flow-accelerated corrosion in field applications. Their tests were carried out using a single-phase horizontal pipeline, rotating cylinders, and jet-impingement techniques. They showed that corrosion rates measured from rotating cylinders could be much less than those from the flow system and the impinging-jet method. Further, a relation between the rate of corrosion and the wall shear stress was established.

Work in this laboratory has shown that multi-phase flow has a large effect on the corrosion mechanisms. Kanwar and Jepson (1994), and Vuppu and Jepson (1994), conducted studies in a 10-cm diameter high-pressure flow loop and showed that the corrosion rate increased with flow velocity, carbon dioxide partial pressure, and temperature. The corrosion products were affected when oil was flowing. The corrosion materials were loose and could be easily removed by the hydrodynamic forces.

This study outlines on the effect of multi-phase flow on corrosion rates at different carbon dioxide partial pressures and temperatures.

EXPERIMENTAL SETUP

The experimental flow loop is shown in Fig.1. The system is made out of 316 stainless steel that can operate at pressures up to 10MPa. Liquid mixtures are stored in a 1.15-m³ tank which contains a de-entrainment table which helps in the separation of gas and liquid flowing into the tank. A thermostat connected to two heaters in the tank maintain a preset temperature. The liquid is pumped from the tank by a 5-kW centrifugal pump into a pipe, 7.5cm internal diameter where the flow rate is measured by an orifice plate. The liquid then passes into a 10-cm internal diameter pipeline. The system is pressurized with carbon dioxide and, if necessary, gas is bubbled into the pipe at point F on the 10-cm pipe. The multi-phase mixture then flows through the test section and back into the tank, where the gas and liquid are separated. The gas is vented and the liquid mixture recycled.

The test section is shown in Fig.2. Corrosion measurements were made using electrical resistance (ER), linear-polarization resistance (LPR) probes, and metal coupons made out of 1018 carbon steel. It was found that the LPR probes did not function well at high oil concentrations. Their use was limited to oil concentrations up to 20%. The ER probes and metal specimens were used to measure the corrosion at the pipe wall for all conditions. Since the corrosion rates of the pipe wall are being measured, the probes and coupons were inserted into the pipe at the positions C and E and are flush mounted.

The sampling tube, ST, has a dual purpose. It is used to determine the variation of the flowing void and oil/water fractions across a vertical diameter and to measure the oxygen content, pH, and dissolved iron in the system. Several pressure tappings (P), connected to a pressure transducer, measure the pressure gradient. The wall shear stress can be measured using probes positioned at S. However, in this work the shear stress is calculated from the flow velocities.

The liquids used in this study are ASTM saltwater and two oils, Conoco LVT200 and ARCOPAK90. At 40°C, the oils have densities and viscosities of 825 and 850kg/m³ and 2 and 15cp respectively. These oils have similar properties to gas condensate and light oil flows. The saltwater is prepared by dissolving ASTM standard sea salt in a measured quantity of deionized water. The system is then filled with the desired oil/water composition.

The system is then deoxygenated by purging with carbon dioxide. During this procedure, regular checks are made on the oxygen levels, using CHEMets' dissolved-oxygen test kits. The process is continued until the oxygen level is below 30ppb. This procedure is then stopped and the pressure raised to the desired operating level. The iron level in the solution is monitored throughout each experiment, and is kept below 10ppm.

The use of an ER probe generally requires a sufficient length of time before the corrosion measurement stabilizes. This time period is usually between 12 and 36 hours for full pipe flow, depending on the flow conditions.

Carbon dioxide partial pressures of 0.27MPa, 0.45MPa, and 0.79MPa for full pipe flow and slug flow are examined. Oil/water concentrations of 100% water, 80% water - 20% oil, 40% water - 60% oil, 20% water - 80% oil, and 100% oil. These experiments are performed at preset temperatures ranging from 40 and 90°C.

RESULTS

Phase distribution

In the understanding of corrosion in multi-phase pipelines, it is essential to have a thorough knowledge of the various flow patterns that are present at each set of conditions. A schematic outline of the flow regimes for two-phase liquid/liquid and three-phase liquid/liquid/gas flows are presented in Figs 3(a) and 3(b).

Fig.3(a) shows the patterns reported from data collected from small-diameter pipe systems. At low oil flowrates, the oil is entrained in the water and, due to buoyancy forces, is located near the top of the pipe. At higher oil flowrates, a stratified flow occurs with the oil flowing above a water layer. At high water and/or oil velocities, a mixed flow can occur. Here, at high water cuts, water is the continuous phase with oil droplets dispersed in it. At low water concentrations, the phases are reversed, with oil being the continuous phase, etc. An emulsion can also form at these high flowrates. This is not mixed flow, but an homogeneous pseudo-fluid with properties very different from both the oil and water. There is still little understanding of the flow of these emulsions since they can behave like a water phase, an oil phase, or a completely different phase.

For this study in 10-cm diameter pipes, for the full pipe, liquid/liquid flow for liquid velocities up to 2m/s, and pressures as high as 0.79MPa, only a stratified flow was encountered. Only a certain portion of the flow near to the oil/water interface resembled a mixed flow. The thickness of this mixed zone did increase with an increase in velocity.

Fig.3(b) shows the flow regimes for gas/liquid/liquid flows. These are very similar to those encountered in two-phase gas/oil flows. The main difference is the presence of a water layer at the bottom of the pipe for stratified and wavy flow. At low gas and high liquid velocities, plug flow occurs. In three-phase flow, the plug is usually all oil which "skates" over the water film. The water layer is virtually unaffected by the passage of the plug.

As the gas velocity is increased, slug flow occurs. The flow in the mixing zone of the slug and inside the slug body seems to be well mixed at the higher slug velocities. However, between slugs, it was found that the stratified film is not a mixed flow of oil and water but stratifies into two separate oil and water layers. This was even for high gas velocities.

For the annular flow regime, the oil and water phases were well mixed with no appearance of separate layers.

Effect of flow on corrosion

a) Full pipe liquid/liquid flow

The results for 20% ARCOPAK90 oil and 80% saltwater at a temperature of 40°C are given in Fig.4. At a liquid flow velocity of 0.28m/s, the corrosion rates at partial pressures of 0.27, 0.45, and 0.79MPa are 4.2, 7.9, and 11.2mm/yr respectively. These results show that the corrosion rate increases substantially with an increase in partial pressure of carbon dioxide. Increasing liquid velocity also increase corrosion rate. This may be due to the increased wall shear stress and turbulence levels. Similar results are noted for all the oil/water compositions up to 60% oil.

The De Waard and Lotz (1993) predictions for the same flow conditions are also included in Fig.4. In each case, their calculated corrosion rates are always much lower than the experimental value. The difference decreases at higher liquid velocities.

Fig.5 shows the variation of corrosion rate with oil/water fraction for ARCOPAK 90. At a carbon dioxide partial pressure of 0.79MPa and a liquid flow velocity of 1m/s, corrosion rates for 0, 20, and 60% oil are 11.4, 13.4 and 16mm/yr respectively. Similar results were obtained for Conoco LVT200 oil and these are shown in Fig.6. In each case for both oils, the corrosion rate had decreased rapidly to very low values above 60% oil. The continued high levels of corrosion at 60% oil was surprising. Results from vertical flows indicate that the sudden decrease in corrosion rate occurs at oil compositions between 25 and 40% oil. Here, the oil and water phases are always well mixed and,

above 20% oil, the oil makes contact with the pipe wall providing some protection against corrosion.

However, on close examination of the distribution of the phases obtained from the sampling tube, it became apparent, as described above, that the oil and saltwater do separate, resulting in a relatively-thick water film at the bottom of the pipe. Thus, for oil compositions up to 60%, the bottom of the pipe is in contact with the water and this results in the high rates of corrosion. However, at higher oil percentages, the phases become well mixed or phase inversion occurs, and this results in oil replacing the water at the bottom of the pipe. This leads to the sudden decrease in the corrosion rate.

The effect of temperature on corrosion rate is shown in Figs 7, 8, 9, and 10. Fig.7 compares the corrosion rate variation with that predicted by de Waard and Milliams at pressures of 0.27 and 0.79MPa for saltwater alone. It can be seen that at each pressure, the corrosion rate increases with temperature up to approximately 60°C. Between 60 and 80°C, the corrosion starts to decrease. This has been shown by de Waard to be due to the formation of iron carbonate layers at the pipe wall which are protective. He predicts the maximum corrosion rate to be within the range of 60 to 80°C. However, the predicted corrosion rates are somewhat lower than the experimental values of this study.

When oil is present, the experimental results show that the maximum in the corrosion rate does not occur for temperatures up to 80°C. This is illustrated in Fig.8. The corrosion rate continues to increase with temperature. Examination of coupons under a scanning electron microscope shows that, when oil is present, the corrosion products do not form a uniform protective layer of carbonate. Many cracks and voids are noted in the layer which allows corrosion to continue.

This is seen at all oil concentrations up to 60% oil, as shown in Figs 9 and 10. The corrosion rate increases with increase in temperature for temperatures up to 80°C.

b) Corrosion under slug-flow conditions

It has been shown by Sun and Jepson (1992), and Zhou and Jepson (1993), that high levels of wall shear stress are encountered in the mixing zone of the slug, and these depend on the Froude number in the liquid film ahead of the slug. A typical shear-stress variation is given in Fig.11 where the Froude number is defined as:

$$Fr = (V_t - V_f)/(g \cdot h_f) \quad (1)$$

where V_t = translational velocity of the slug front
 V_f = average velocity of the liquid film
 g = acceleration due to gravity
 and h_f = effective height of the liquid film.

As the Froude number is increased, the average wall shear stresses increase dramatically from values of 22Pa at a Froude number of 6 to 140Pa at a Froude number of 12. The turbulence levels also increase with increase in Froude number. These values are much higher than any typical full-pipe or stratified-type flows.

The effect of slug flow on corrosion rate is shown in Fig.12. The oil used is the light condensate, LVT 200 oil at a pressure of 0.13MPa and a temperature of 40°C. In it is clearly indicated that, at each composition, increasing the Froude number increases the corrosion rate. It can be again noted that increasing oil composition does not lead to much lower corrosion rates. For slug flow with this oil, there is still a corrosion rate of 1mm/yr at an oil percentage of 80% and a Froude number of 12.

From analysis of high-speed video tapes of the flow mechanisms, it was noticed that pulses of bubbles are formed at the front of the slug in the mixing zone. These are seen to be forced towards the bottom of the pipe and, at high Froude numbers, actually impacting on the pipe. Fig.13 relates the corrosion rate to the amount of gas present at the bottom of the pipe for the same conditions as those in Fig.12. At each water cut, there is a higher corrosion rate when more gas is present.

The effectiveness of several corrosion inhibitors were studied under slug-flow conditions. Some did not reduce the corrosion rate significantly. Coupons from these tests were studied using a

scanning electron microscope and destruction of the inhibitor film was noticed. Evidence of this is shown in Fig. 14 which is for slug flow with a Froude number of 12 using the LVT 200 oil. Circular holes of approximately 0.1 mm diameter are found in the inhibitor film. Within these holes, there are signs of corrosion product removal and continued high levels of corrosion. It is suggested that these are caused by the impact and subsequent collapse of the gas bubbles as they hit the bottom of the pipe. Evidence of these bubble impact points has also been noticed by Xia *et al.* (1989) for stagnant gas bubbles attached to a steel surface.

Further evidence of bubble collapse is provided in Fig. 15. This shows the raw data of the change of wall shear stress with time. It can be seen that large pulses in the shear stress appear at regular intervals of approximately 0.4 seconds at this Froude number of 12 for 80% saltwater and 20% oil. Instantaneous values of shear stress of 75 Pa are seen. At higher oil percentages, shear stresses as high as 1000 Pa have been recorded. From a preliminary study of the flow, the frequency of these pulses is very similar to the frequency of the pulses of bubbles produced in the mixing zone of the slug.

At a higher pressure of 0.47 MPa, the corrosion rate for slug flow with saltwater only at a Froude number of 6 has increased to 6 mm/yr at 40°C. The effect of increasing temperature at these conditions is presented in Fig. 16. The corrosion rate increases substantially with temperature and, at 90°C, the corrosion rate has risen to 46 mm/yr. Rates as high as these have been reported from field trials when the water cut is high.

CONCLUSIONS

From the results of this study it is clearly demonstrated that a knowledge of the types of flow encountered in multi-phase pipelines is essential to obtain a proper understanding of the corrosion processes. The flow regimes, especially slug flow, have a large effect on the corrosion mechanisms. These are not seen in any single-phase flow systems, stirred beakers, and rotating-cylinder electrodes.

For almost all the conditions studied there was a water layer present at the bottom of the pipe in horizontal flow. This is not noticed in vertical flows at the same flowing conditions.

In slug flow, large regions of high shear stresses and turbulence have been found. Instantaneous values of wall shear stresses as high as 1000 Pa were recorded. These correspond to pulses of bubbles being formed in the mixing zone at the front of the slug, which then impact on the bottom of the pipe. Here, evidence of bubble collapse was noted.

For the oils tested, the corrosion rates were found not to change much with an increase in oil concentration up to 60% oil. This can be attributed to the separation and stratification of the oil and water in the pipe which formed a water layer at the bottom of the pipe. However, above 60% oil, the corrosion rate decreased rapidly and is negligible at 80% oil.

The corrosion rates increased with an increase in liquid flow velocity for oil percentages up to 60%. Higher rates of shear and increased turbulence are present at the higher velocities and can contribute to the enhanced corrosion rates.

Increasing partial pressure of the carbon dioxide led to large increases in the corrosion rates. The De Waard and Lotz (1993) equations seem to under-predict the corrosion rate by a factor of approximately 2.

For brine only, as the temperature is increased, the corrosion rate increased to a maximum between 60 and 80°C. This corresponds well with that predicted by de Waard. However, when oil is present this maximum is not noticed for temperatures as high as 90°C. The corrosion products are distributed differently when oil is flowing.

For slug flow, even for brine alone, no maximum corrosion rate is found for tests up to 90°C.

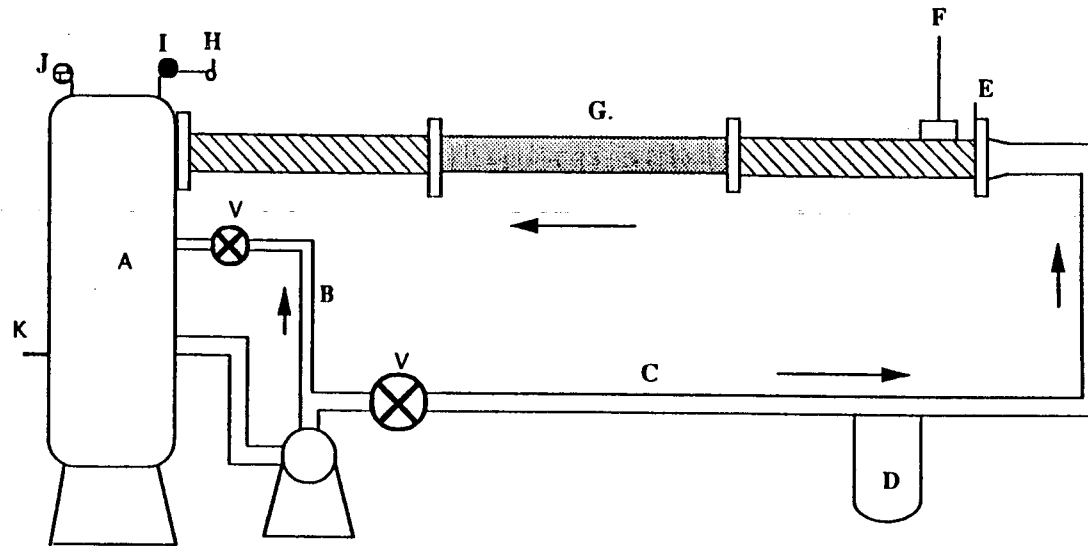
The pulses of bubbles found in the slug front do impact on the bottom of the pipe. In the corresponding regions of high wall shear forces, bubble collapse leads to high rates of corrosion. Further, at these locations, holes in inhibitor films have been found and these do not repair with time.

Many tests on the effectiveness of inhibitors do not subject the inhibitors to this type of flow behavior. Consequently, inadequate results are often obtained.

REFERENCES

1. De Waard, C., & Lotz, U. (1993). Prediction of CO₂ corrosion of carbon steel. *Corrosion*/93, 50, 69/1-69/17.
2. De Waard, C., Lotz, U., & Milliams, D. E. (1991, December). Predictive model for CO₂ corrosion engineering in wet natural gas pipelines. *Corrosion*/90, 47(12), 976-985.
3. De Waard, C., & Milliams, D. E. (1975). Carbonic acid corrosion of steel. *Corrosion-NACE*, 31(5), 177-181.
4. Dugstad, A. (1992). The importance of FeCO₃ supersaturation on the CO₂ corrosion of carbon steels. *Corrosion*/92, 49(14), 1-13.
5. Efir, K. D., Wright, E. J., Boros, J. A., & Hailey, T. G. (1993, March 7-12). Experimental correlation of steel corrosion in pipe flow with jet impingement and rotating cylinder laboratory tests. *Corrosion*/93, 50, 81/1-81/21.
6. Efir, K. D., Wright, E. J., Boros, J. A., & Hailey, T. G. (1993, September). Wall shear stress and flow accelerated corrosion of carbon steel in sweet production. 12th International Corrosion Congress: Houston, TX.
7. Green, A. S., Johnson, B. V., & Choi, H. (1989). Flow-related corrosion in large diameter multi-phase flowlines. *SPE*, 20685, 677-684.
8. Kanwar, S. and Jepson, W.P. (1994) A model to predict sweet corrosion of multi-phase flow in horizontal pipelines. Paper No. 94024, *NACE CORROSION/94*, Baltimore.
9. Lee, A-H., Sun J-Y, and Jepson (1993) Study of flow regime transitions of oil-water-gas mixtures in horizontal pipelines. 3rd Int. Conf. ISOPE, Singapore. 6-11 June.
10. Mishra, B., Olson, D. L., Al-Hassan, S., & Salama, M. M. (1992). Physical characteristics of iron carbonate scale formation in pipeline steels. *Corrosion*/92, 48, 13/1-13/11.
11. Videm, K., & Dugstad, A. (1989, March). Corrosion of carbon-steel in an aqueous carbon dioxide environment, Part 1: Solution effects. *Materials Performance*, 63-67.
12. Sun, J-Y, and Jepson, W.P. (1992) Slug flow characteristics and their effect on corrosion rates in horizontal oil and gas pipelines. *SPE* 24787, 215-228
13. Videm, K., & Dugstad, A. (1989, April). Corrosion of carbon steel in an aqueous carbon dioxide environment, Part 2: Film formation. *Materials Performance*, 46-50.
14. Vuppu, A.K., and Jepson, W.P. (1994) Study of sweet corrosion in horizontal multi-phase, carbon steel pipelines. OTC paper 7494, 26 Annual Offshore Technology Conference, Houston Texas, 2-5 May.
15. Xia, Z., Chou, K-C, and Smialowska, S.Z (1989) Pitting corrosion of carbon steel in brine containing carbon dioxide. *CORROSION*, 45(8), 636,642.
16. Zhou, X. and Jepson, W.P. (1993) Corrosion in three-phase oil/water/gas slug flow in horizontal pipes. Paper No. 94026, *NACE CORROSION/94*, Baltimore.





- | | |
|---|---|
| A. Liquid Tank | G. Test Section - 10.16 cm Stainless Steel Pipe |
| B. Liquid Recycle | H. Gas Outlet with filters |
| C. Liquid Feed - 7.62 cm Stainless Steel Pipe | I. Pressure Gauge with Back Pressure Control |
| D. Orifice Plate with a Pressure Transducer | J. Safety Valve |
| E. Flow Height Control Gate | K. Heater |
| F. Carbon dioxide Feed Line | V. Flow Control Valves |

Figure 1. Experimental System

- E - ER Probe or LPR Probe
- C - Coupon
- P - Pressure Tappings
- S - Shear Stress Probe
- ST - Sampling Tube
- V - Void Fraction Tube

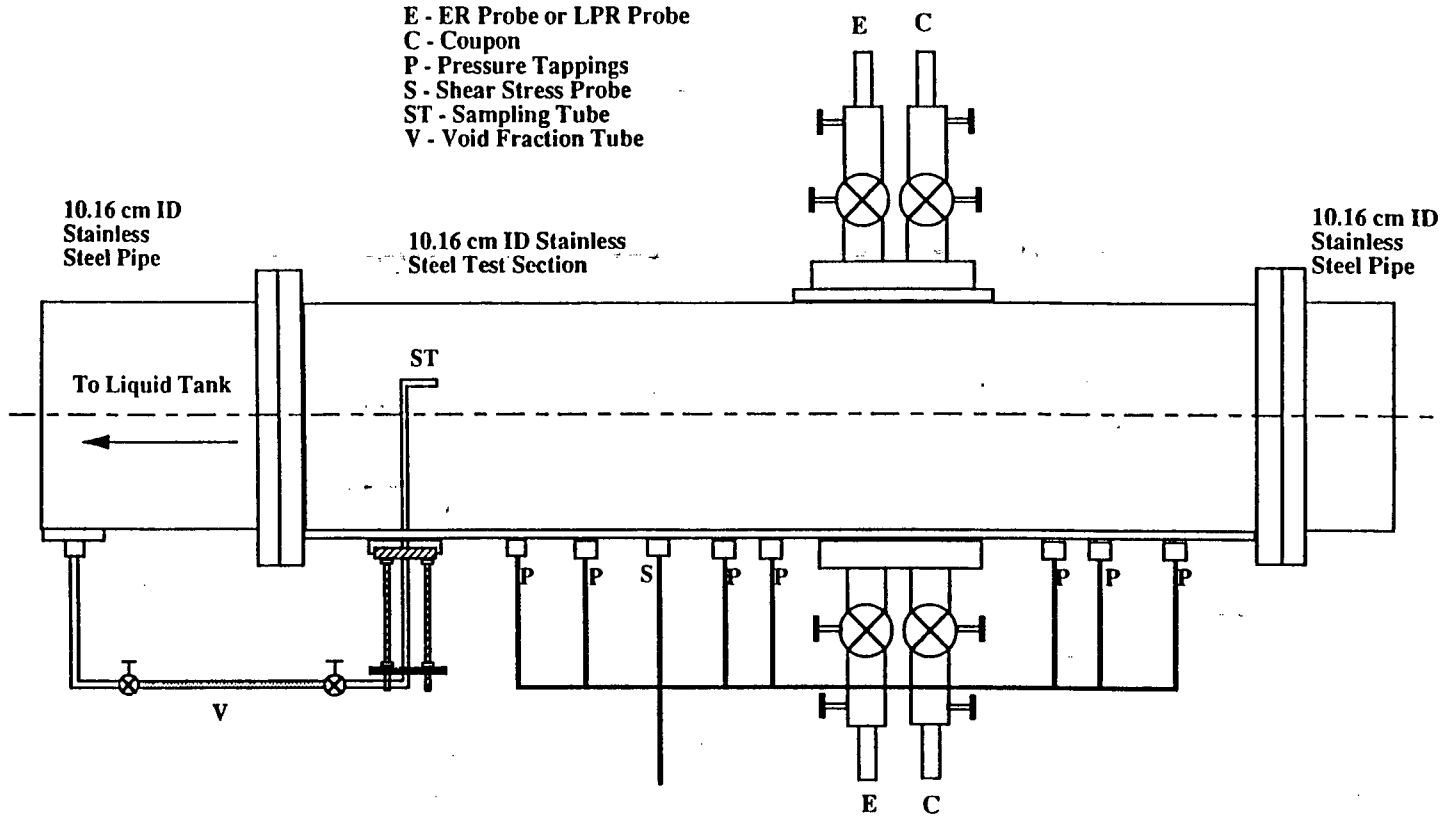
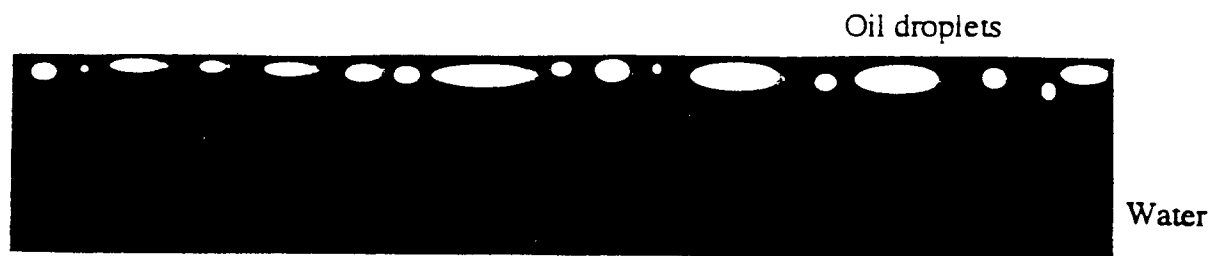
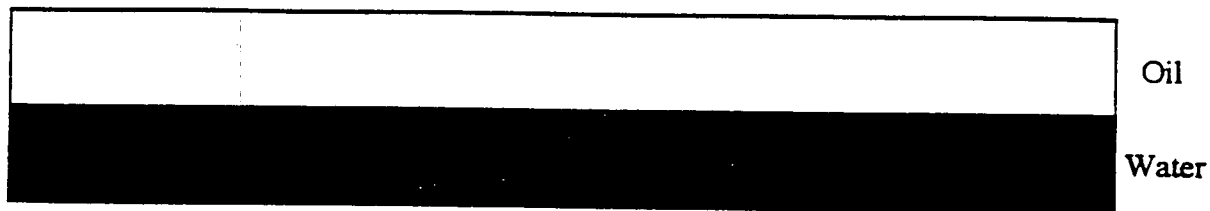


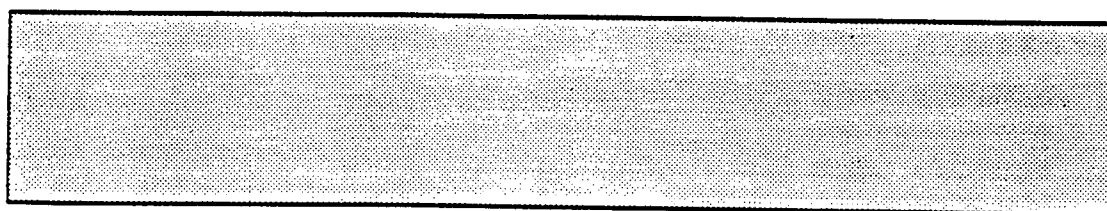
Figure 2. Test Section



Bubble Flow



Stratified Flow



Mixed Flow

Figure 3(a). Flow patterns for oil-water system

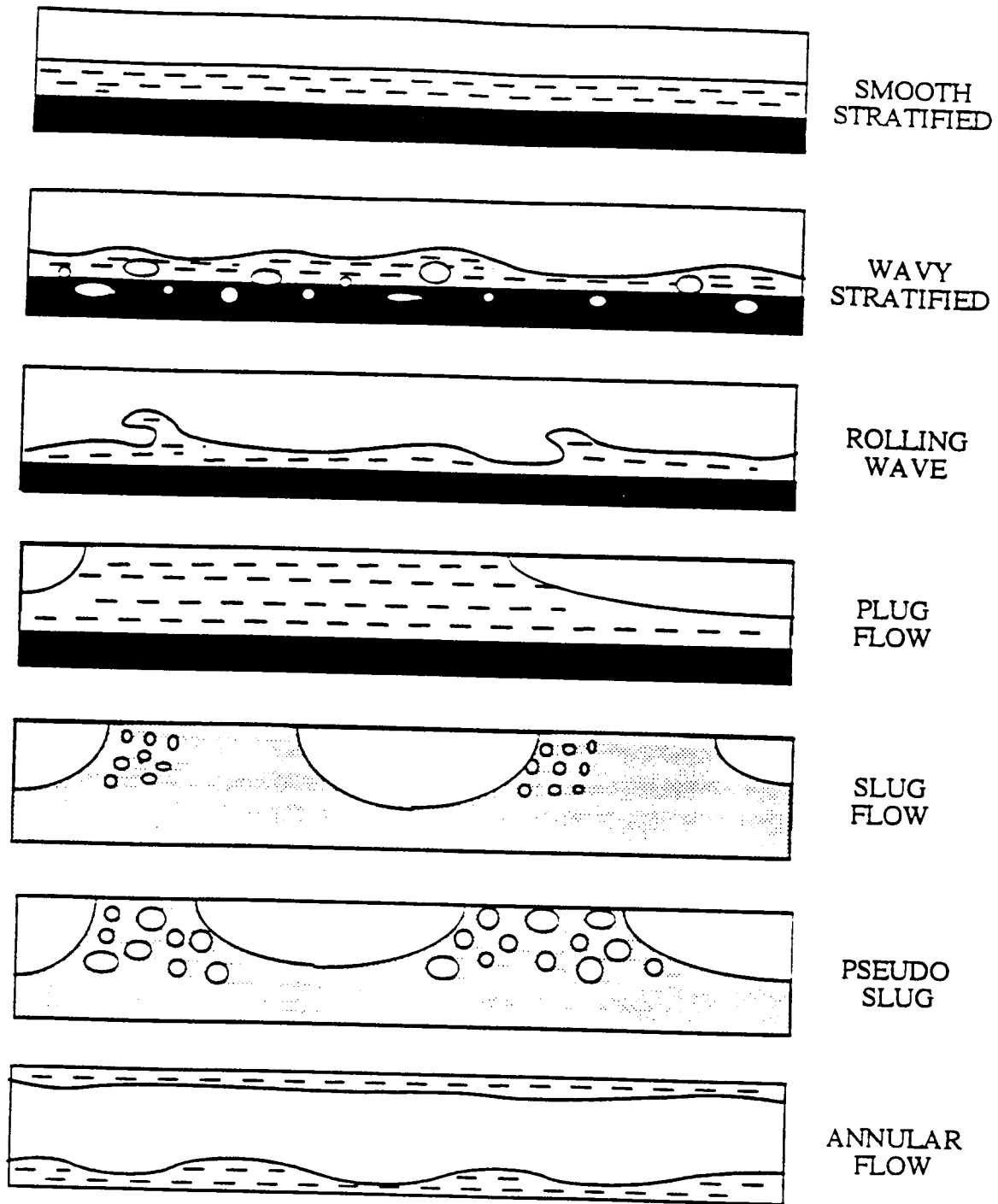


Figure 3 (b): Flow patterns in water-oil-gas mixture flow

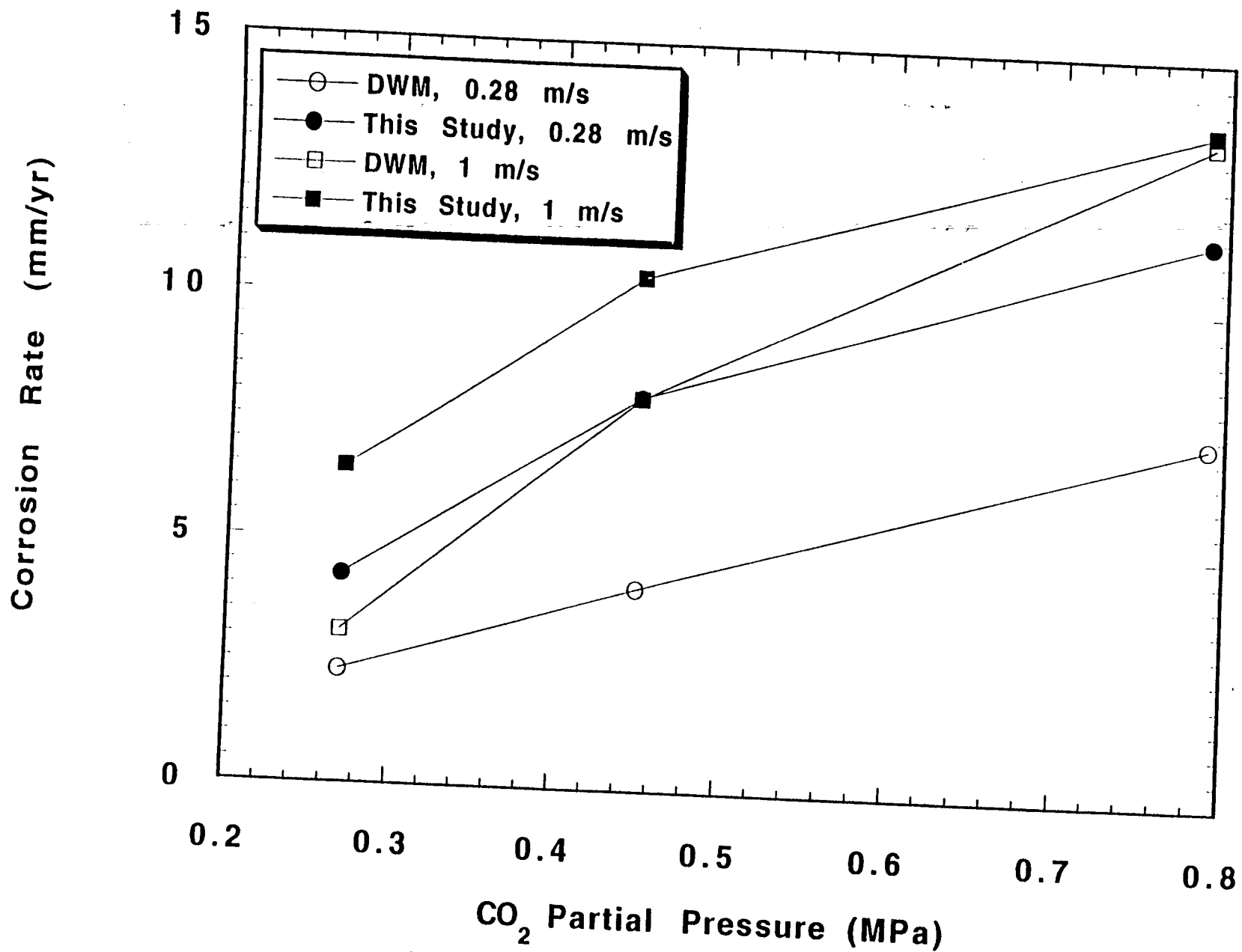


Figure 4. Corrosion Rate Vs CO₂ Partial Pressure
Comparison of DeWaard & Milliams correlation

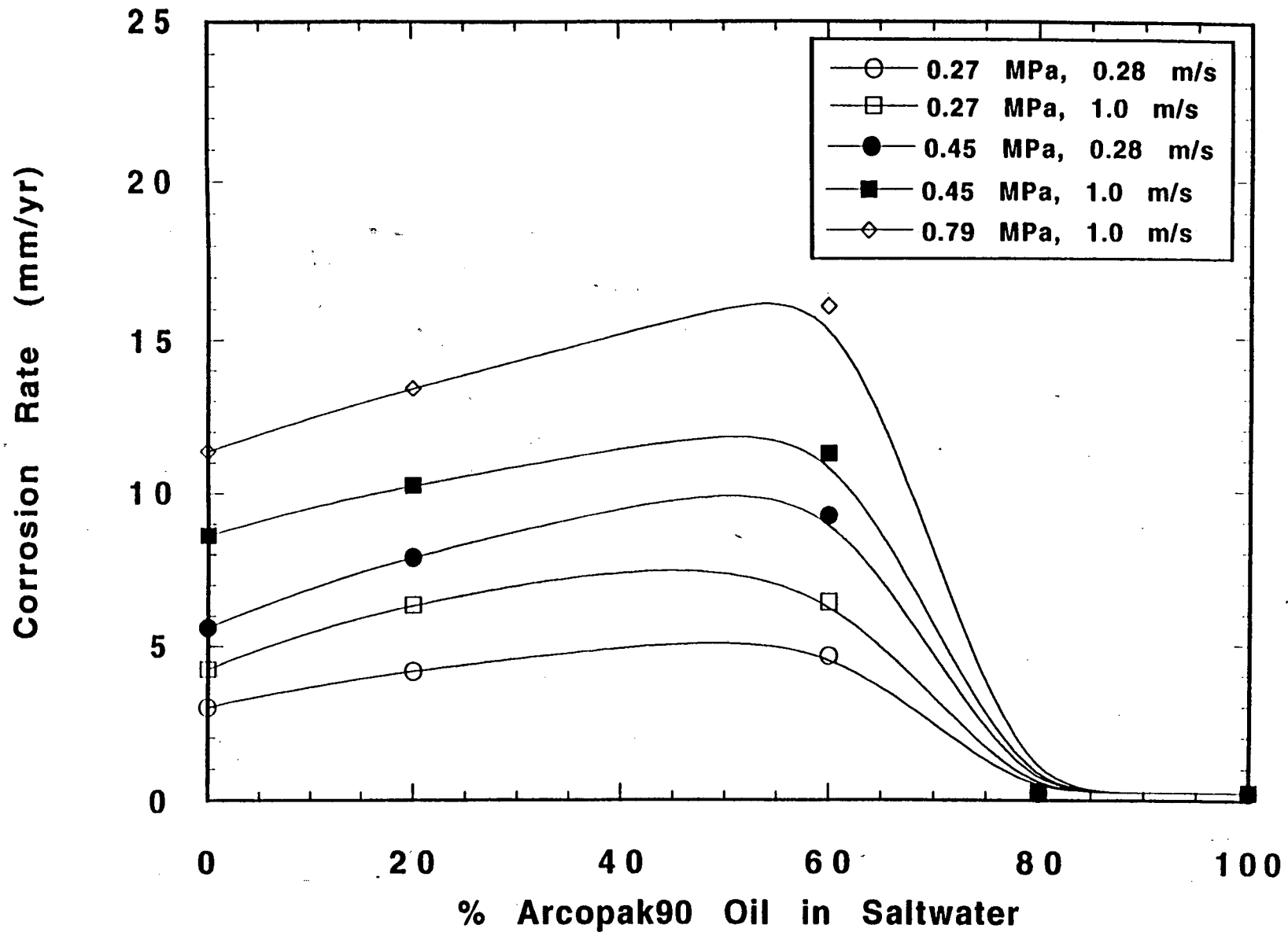
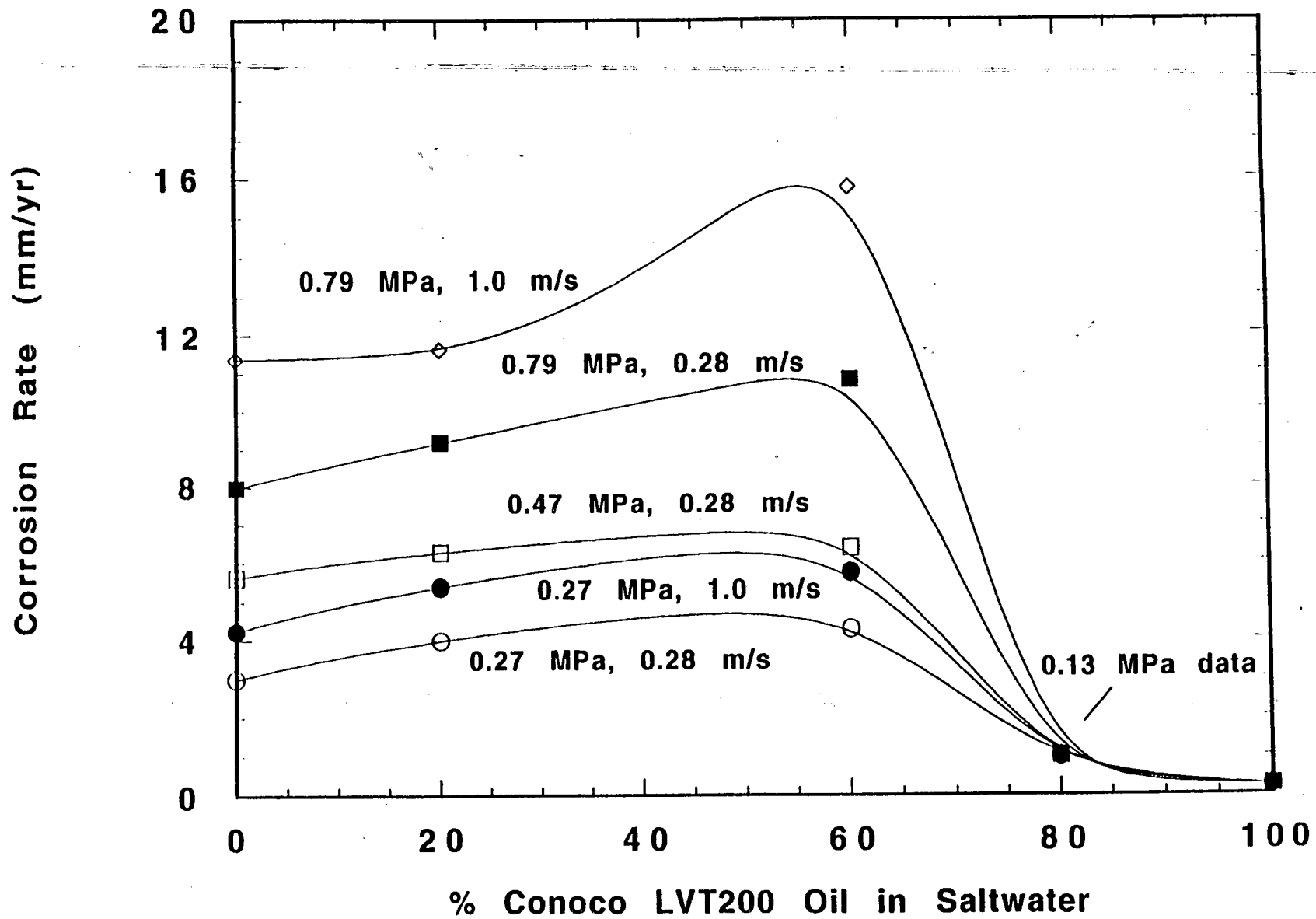


Figure 5. Corrosion Rate vs Oil Concentration
Full Pipe Flow



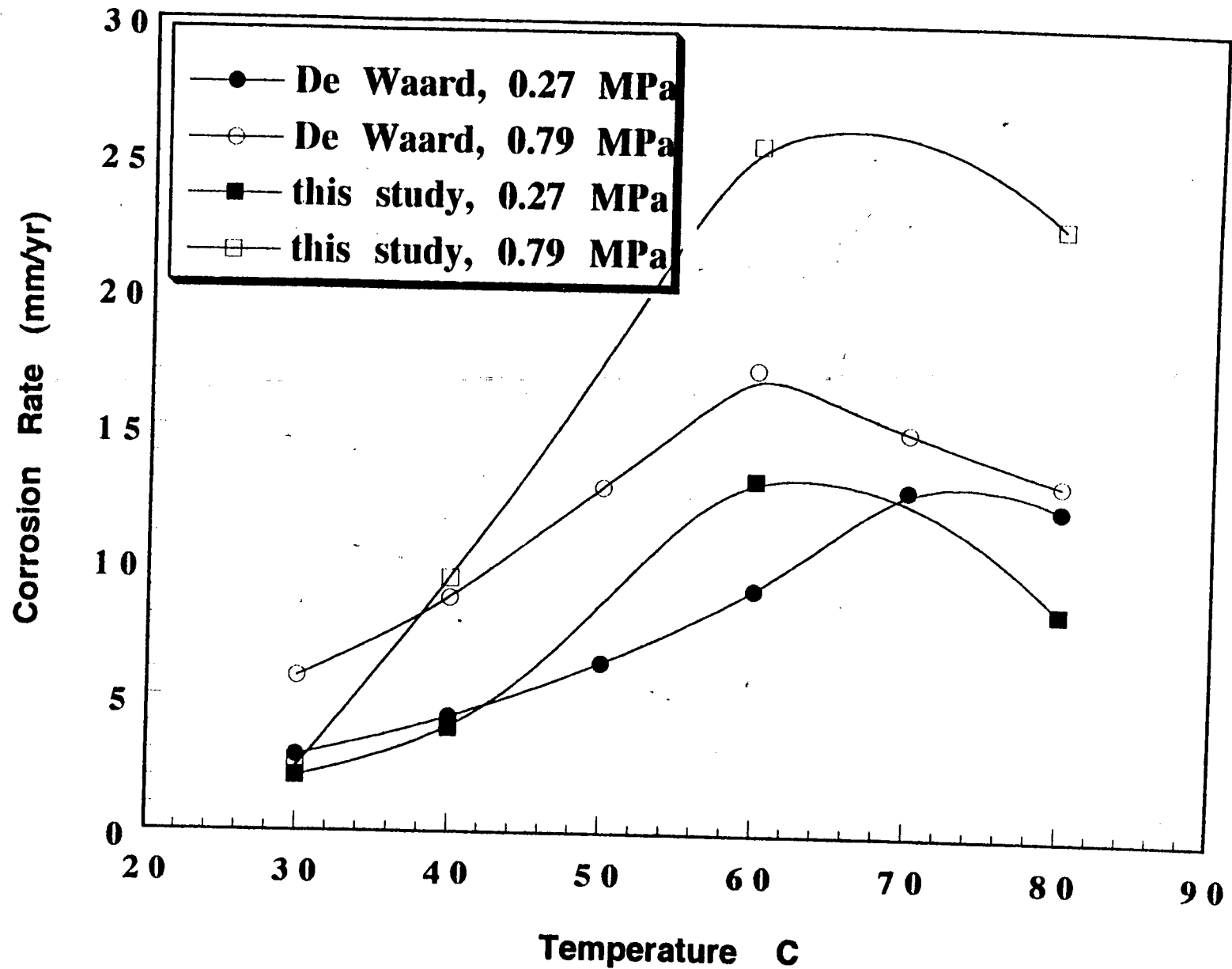


Figure 7. Plot of Corrosion Rate vs Temperature for full pipe flow of Salt Water at 1 m/s

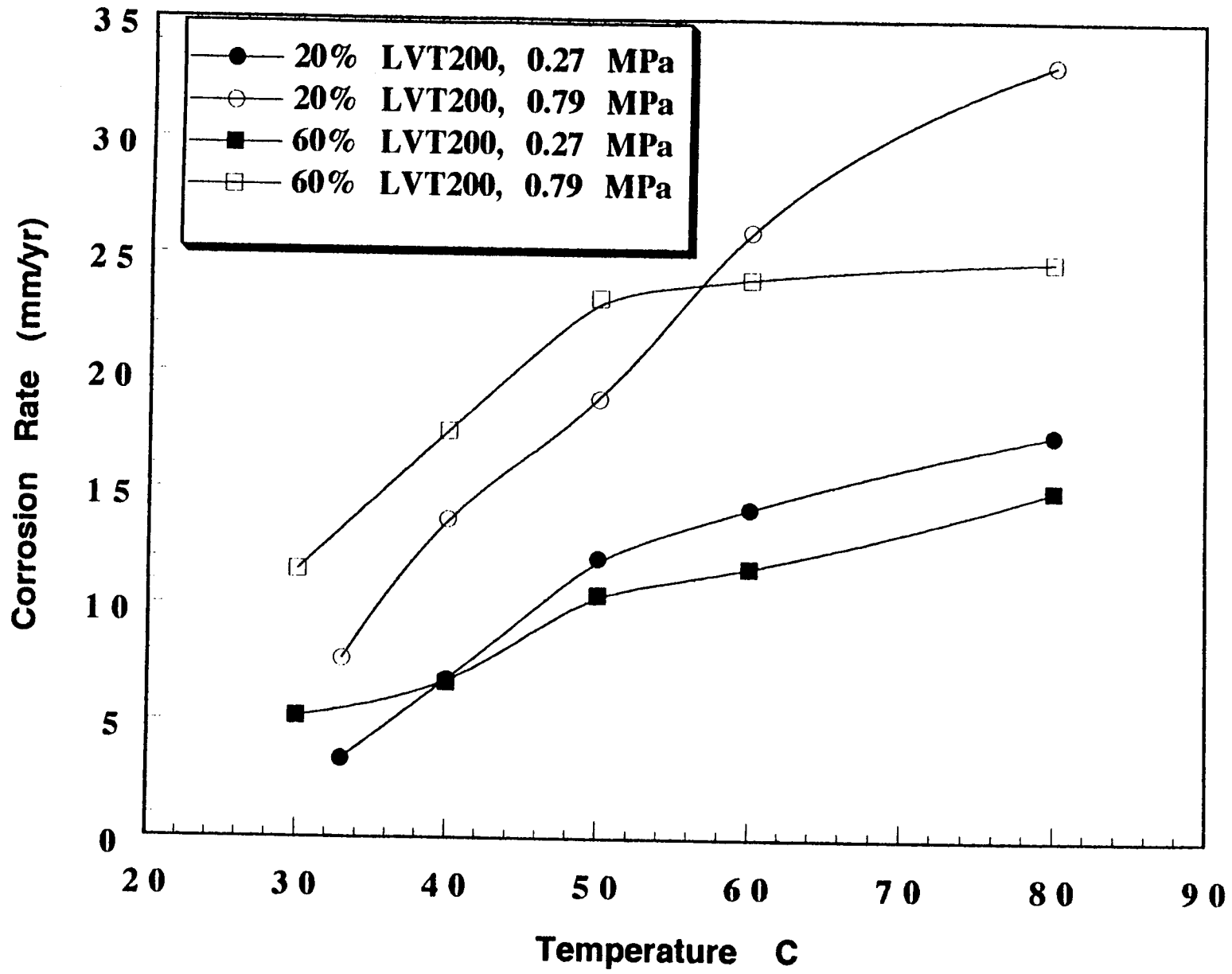


Figure 8. Plot of Corrosion Rate vs Temperature for full pipe flow of Conoco LVT200 Oil/Water mix at 1 m/s

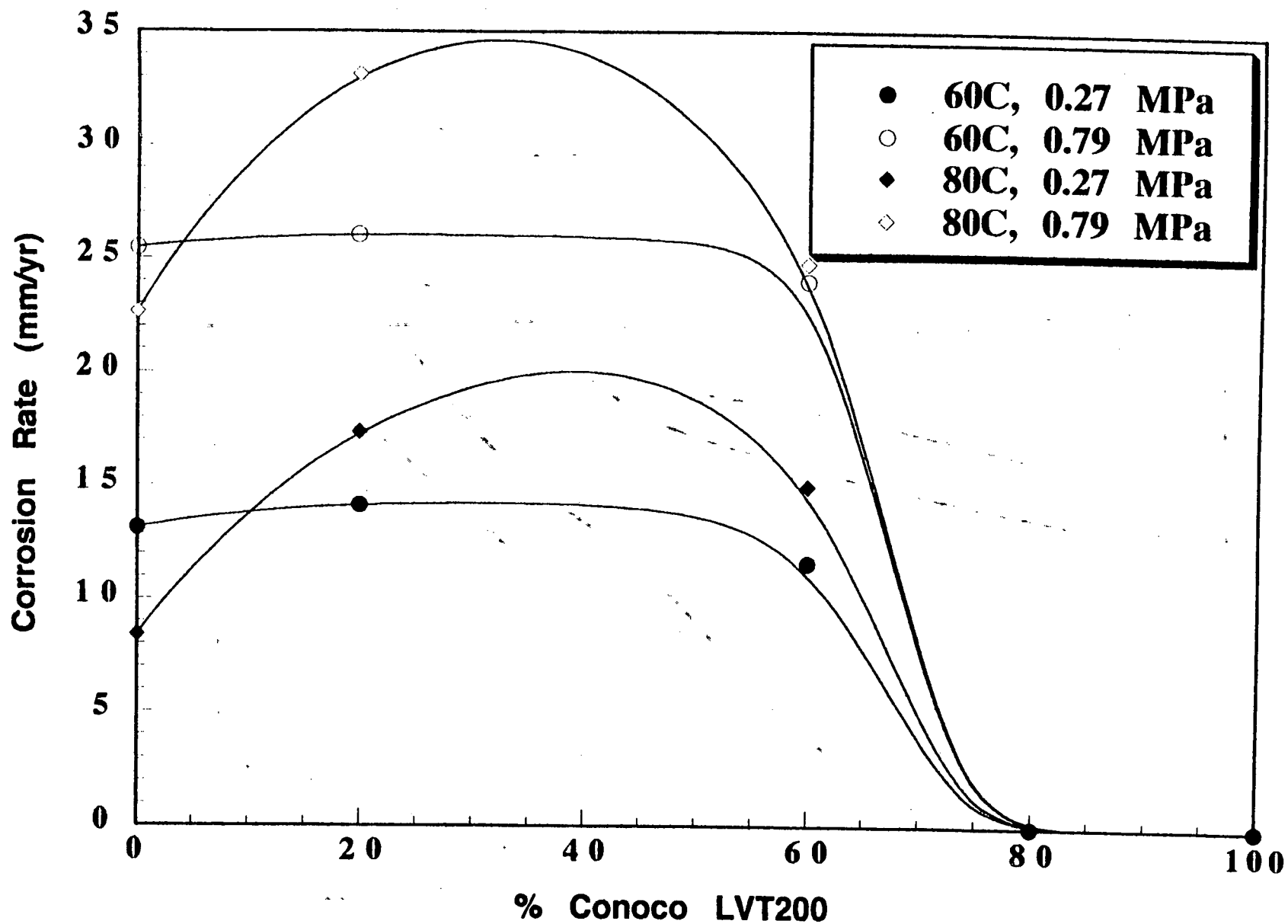


Figure 9. Plot of Corrosion Rate vs % Oil fraction for full pipe flow at 60C and 80C and 1 m/s

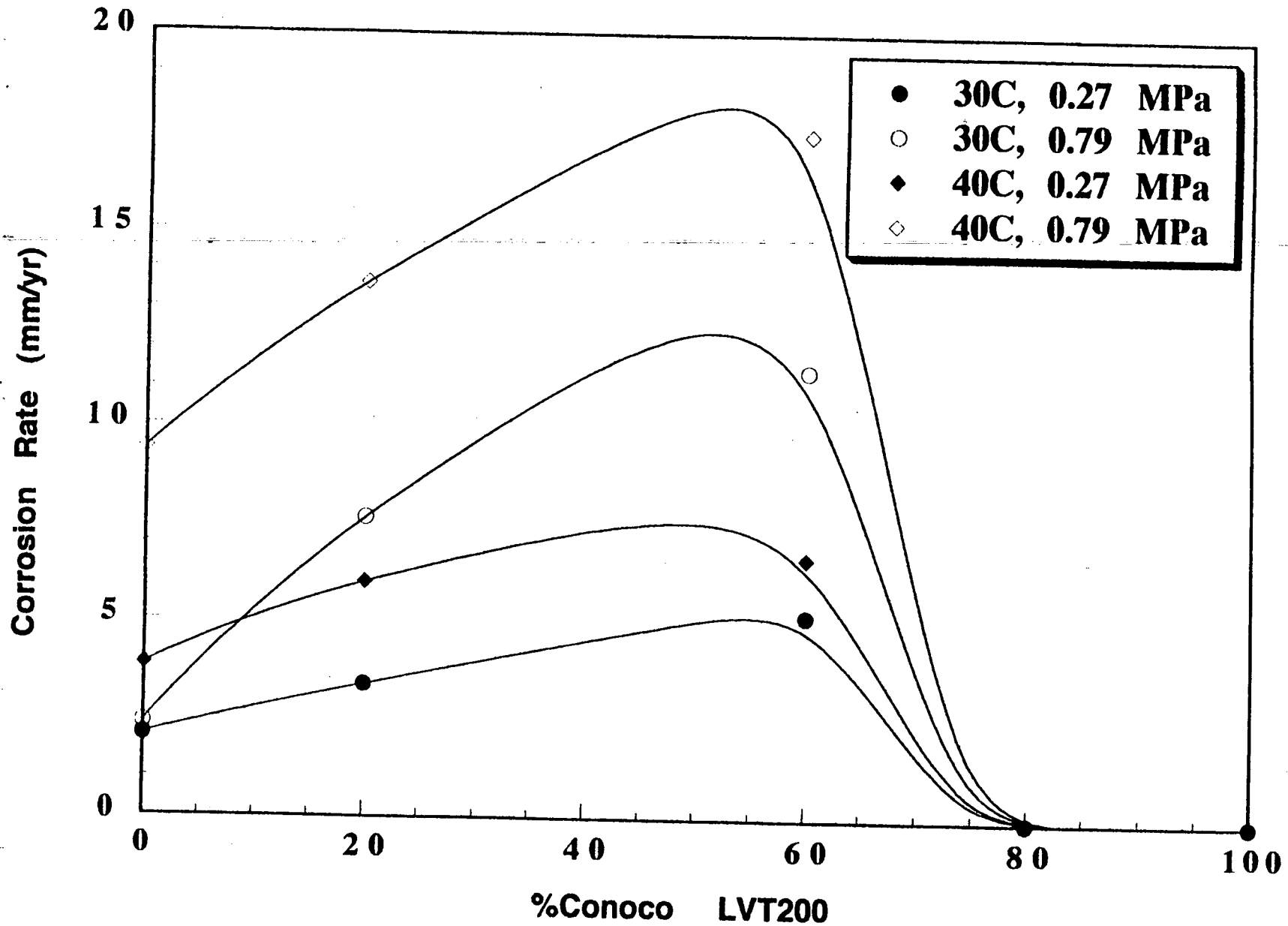


Figure 10. Plot of Corrosion Rate vs % Oil fraction for full pipe flow at 30C and 40C and 1 m/s

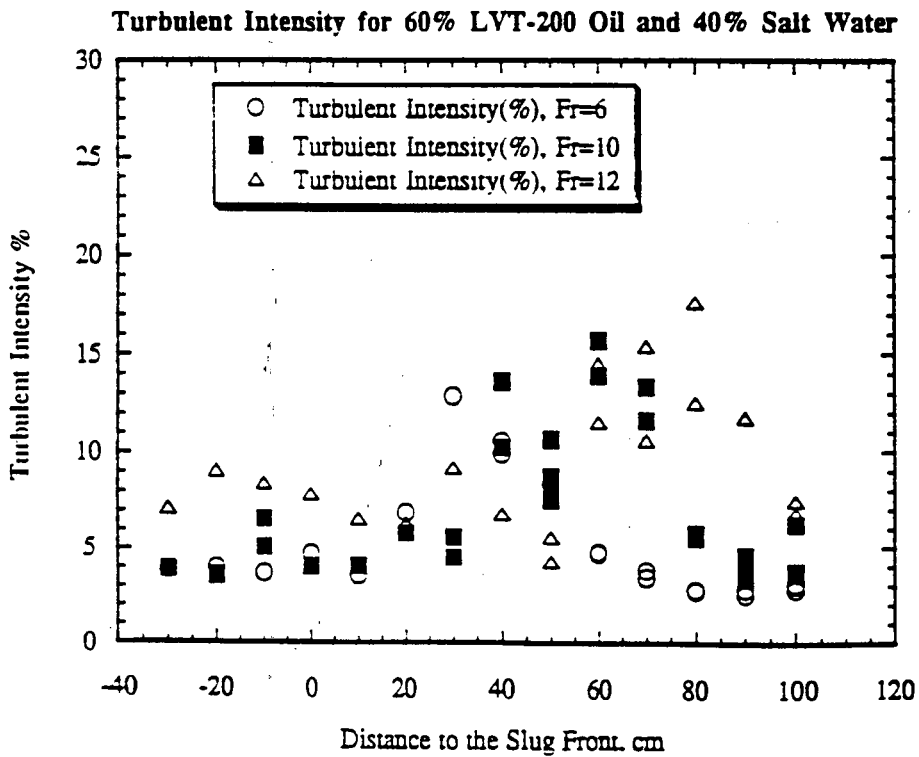
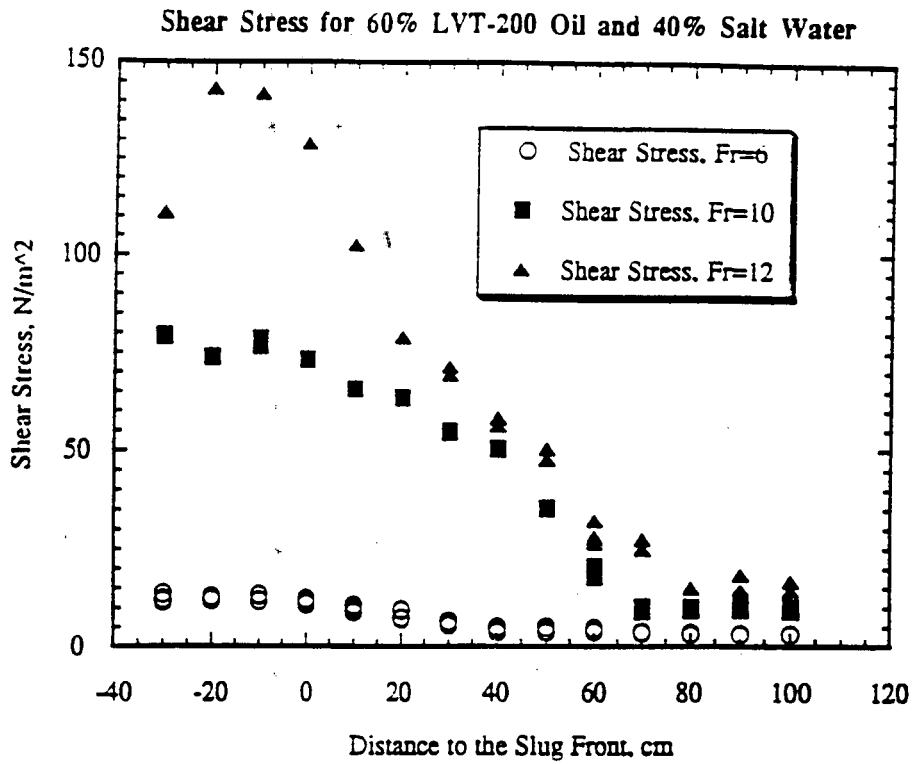


Figure 11. Shear stress and turbulence variation in the slug front.

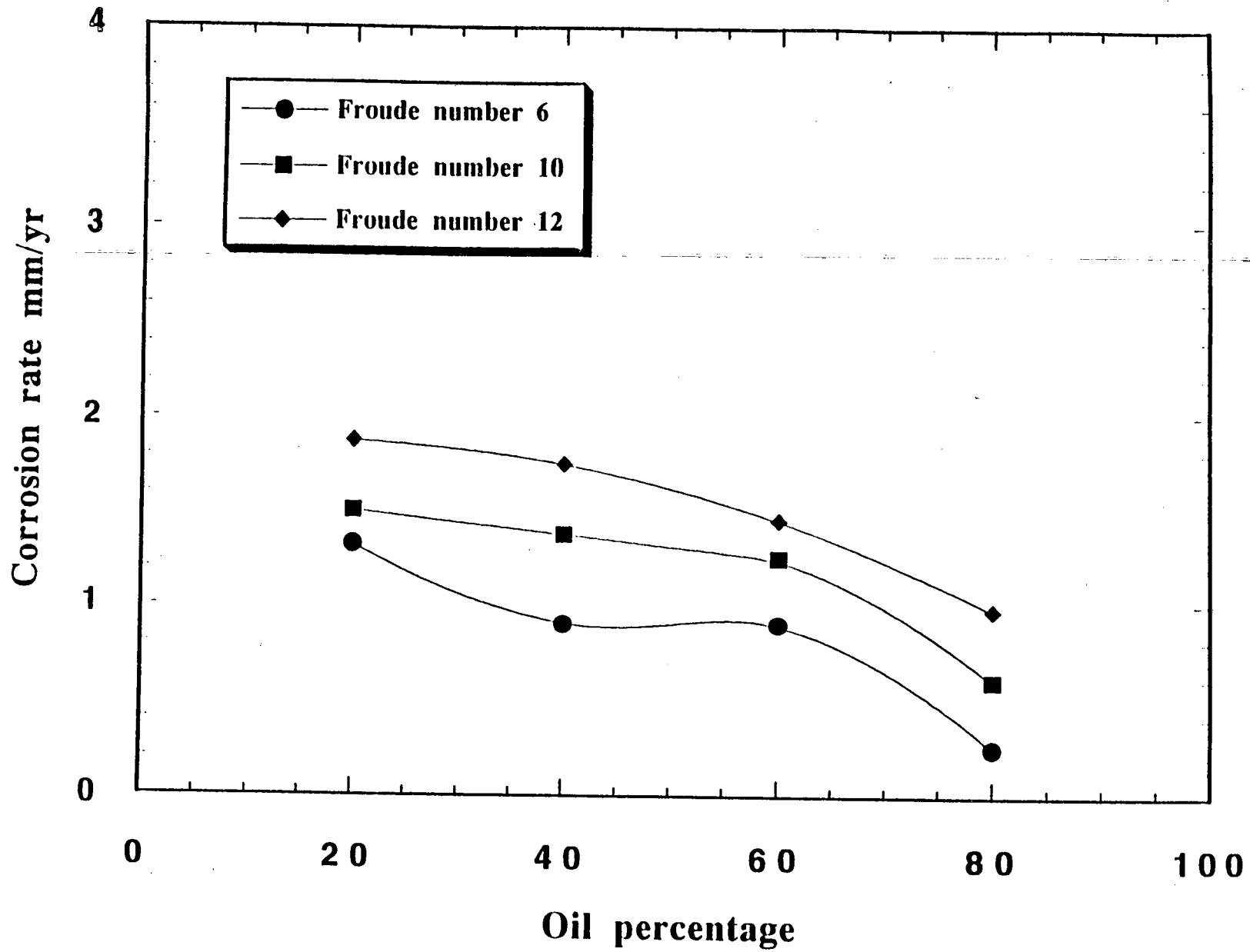


Figure 12. Effect of oil composition on corrosion rate.

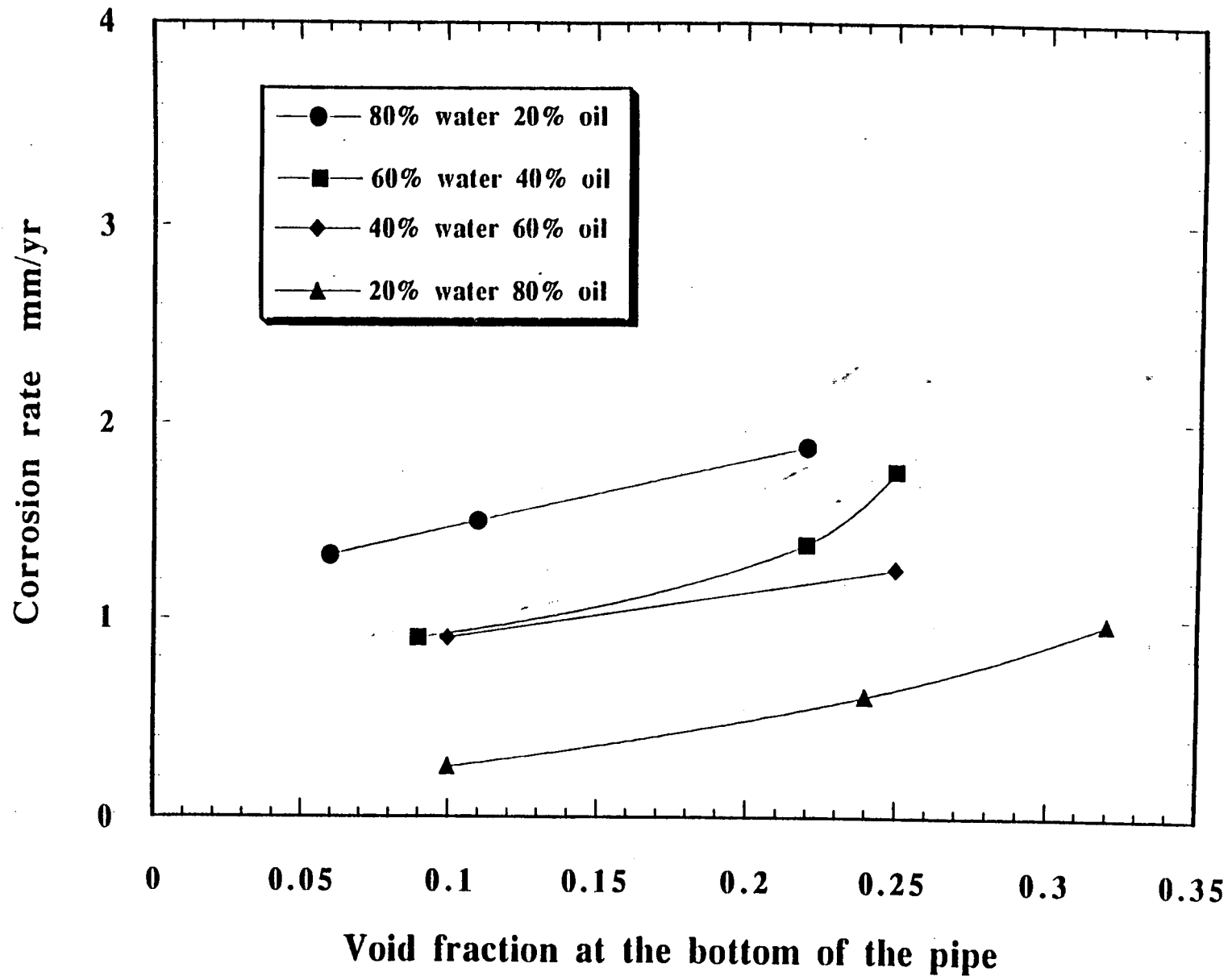
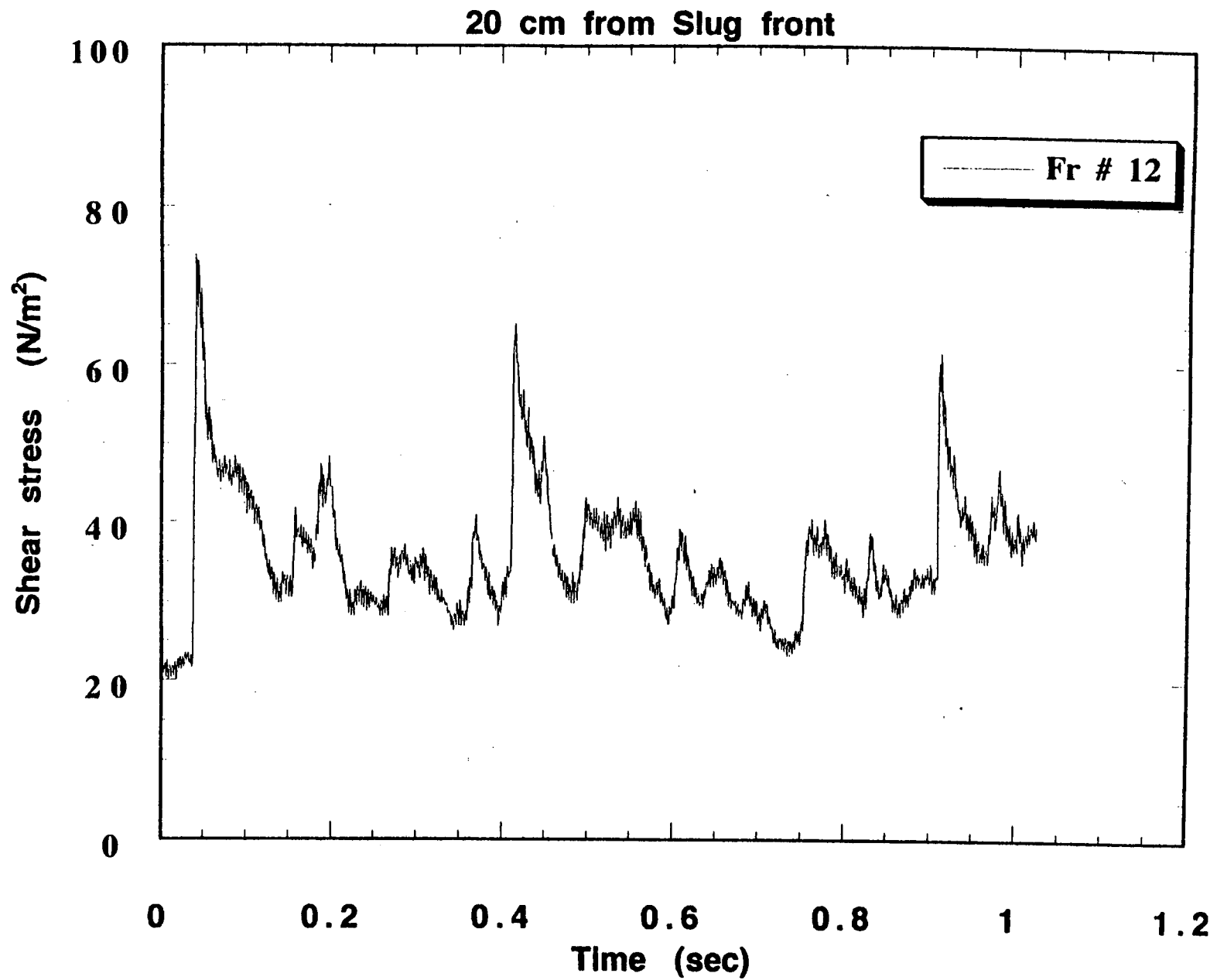


Figure 13. Effect of void fraction at the bottom of the pipe on corrosion rate.



Figure 14. Evidence of bubble impact.



**Figure 15. Instantaneous shear stress
Salt water (80%), LVT200 oil (20%)**

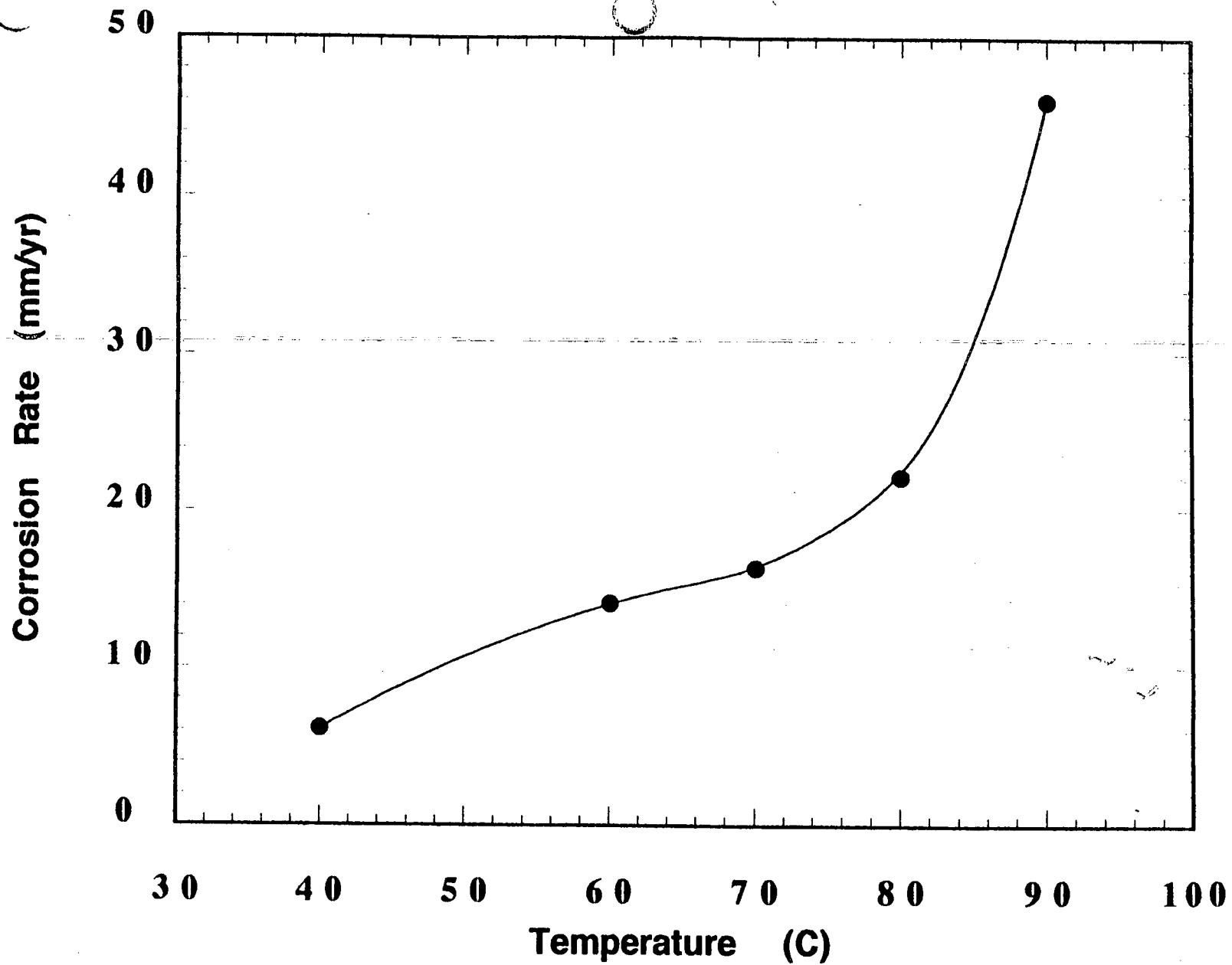


Figure 16. Corrosion Rate vs Temperature for salt water at 0.35MPa and Froude number 6.

